Available online at www.sciencedirect.com
SCIENCE DIRECT®
Geochimica et Cosmochimica Acta 70 (2006) 3436–3448
Geochimica
www.elsevier.com/locate/gca

Search for nucleosynthetic and radiogenic tellurium isotope anomalies in carbonaceous chondrites

Manuela A. Fehr [a,b,*], Mark Rehkämper [a,c], Alex N. Halliday [a,d], Maria Schönbächler [a,e], Bodo Hattendorf [f], Detlef Günther [f]

[a] ETH Zürich, Institute of Isotope Geology and Mineral Resources, 8092 Zürich, Switzerland
[b] Swedish Museum of Natural History, Laboratory for Isotope Geology, Box 50007, 104 05 Stockholm, Sweden
[c] Department of Earth Science and Engineering, Imperial College, London, SW7 2AZ, UK
[d] Department of Earth Sciences, Oxford University, Parks Road, Oxford OXI 3PR, UK
[e] DTM, Carnegie Institution of Washington, 5241 Broad Branch Road, NW, Washington, DC 20015, USA
[f] ETH Zürich, Laboratory of Inorganic Chemistry, 8093 Zürich, Switzerland

Received 25 July 2005; accepted in revised form 19 April 2006

Abstract

Tellurium isotope data acquired by multiple-collector inductively coupled plasma-mass spectrometry (MC-ICPMS) are presented for sequential acid leachates of the carbonaceous chondrites Orgueil, Murchison, and Allende. Tellurium isotopes are produced by a broad range of nucleosynthetic pathways and they are therefore of particular interest given the isotopic anomalies previously identified for other elements in these meteorites. In addition, the data provide new constraints on the initial solar system abundance of the *r*-process nuclide ^{126}Sn, which decays to ^{126}Te with a half-life of 234,500 years. The ^{126}Te/^{128}Te ratios of all leachates were found to be identical, within uncertainty, despite variations in ^{124}Sn/^{128}Te of between about 0.002 and 1.4. The data define a ^{126}Sn/^{124}Sn ratio of $<7.7 \times 10^{-5}$ at the time of last isotopic closure, consistent with the value of $<18 \times 10^{-5}$ previously reported for bulk carbonaceous chondrites. How close this is to the initial ^{126}Sn/^{124}Sn ratio of the solar system depends on when the investigated samples last experienced redistribution of Sn and Te. No clear evidence is found for nucleosynthetic anomalies in the abundances of *p*-, *s*-, and *r*-process nuclides. The largest effect detected in this study is a small excess of the *r*-process nuclide ^{130}Te in a nitric acid leachate of Murchison. This fraction displays an anomalous ε^{130}Te of $+3.5 \pm 2.5$. Although barely resolvable given the analytical uncertainties, this is consistent with the presence of a small excess *r*-process component or an *s*-process deficit. The general absence of anomalies contrasts with previous results obtained for K, Cr, Zr, Mo, and Ba isotopes in similar leachates, which display nucleosynthetic anomalies of up to 3.8%. The reason for this discrepancy is unclear but it may reflect volatility and more efficient mixing of Te in the solar nebula.

1. Introduction

Nucleosynthetic isotope anomalies in ^{54}Cr (Rotaru et al., 1992; Podosek et al., 1997a), ^{40}K (Podosek et al., 1999), Mo (Dauphas et al., 2002a), Ba (Hidaka et al., 2003), and ^{96}Zr (Schönbächler et al., 2003, 2005) were reported for acid leachates of ordinary and carbonaceous chondrites and it was suggested that these anomalies may be hosted in various types of presolar grains (Alexander, 2002; Dauphas et al., 2002a; Schönbächler et al., 2005) or in unidentified non-acid resistant presolar phases (Podosek et al., 1997a, 1999; Alexander, 2002; Schönbächler et al., 2003, 2005). Tellurium is another element that has considerable potential for the study of such nucleosynthetic isotope anomalies. It has eight stable nuclides, of which ^{120}Te is produced by the *p*-process, ^{122,123,124}Te by the *s*-process, and ^{128,130}Te by the *r*-process. Two isotopes, ^{125}Te and ^{126}Te, are formed by both the *r*- and the *s*-process. Presolar diamonds isolated from the Allende chondrite furthermore exhibit permil to percent level Te isotope anomalies of nucleosynthetic origin (Richter

* Corresponding author. Fax: +46 8 5195 4031.
E-mail address: manuela.fehr@nrm.se (Manuela A. Fehr).

0016-7037/$ - see front matter © 2006 Elsevier Inc. All rights reserved.
doi:10.1016/j.gca.2006.04.019

et al., 1998; Maas et al., 2001). In contrast, recent Te isotope ratio measurements by multiple-collector inductively coupled plasma-mass spectrometry (MC-ICPMS) were unable to identify any Te isotope variations in bulk chondrites and the sulfide and metal fractions of iron meteorites (Fehr et al., 2005).

The primary aim of the present study is to determine whether sequential acid leachates of carbonaceous chondrites exhibit nucleosynthetic Te isotope anomalies. A further goal is the investigation of potential radiogenic isotope effects from the short-lived radionuclide ^{126}Sn, which decays to ^{126}Te with a half-life of 234,500 years (Oberli et al., 1999). This decay system is of particular interest because ^{126}Sn is predominantly an *r*-process nuclide that most likely forms in supernova environments (Qian et al., 1998). The discovery of radiogenic effects from the decay of short-lived nuclides with half-lives of less than 1 Myr (e.g, ^{26}Al, ^{41}Ca) in meteorites requires that these isotopes were produced either within the nascent solar system by spallation or in a late stellar nucleosynthetic event that took place just prior to the collapse of the protosolar cloud (Lee et al., 1998; Meyer and Clayton, 2000). As ^{126}Sn cannot be produced by spallation, the discovery of ^{126}Te excesses that correlate with Sn/Te ratios in meteorites would provide tight time constraints on the formation of the solar system. The presence of former live ^{126}Sn in the early solar system would be in agreement with a supernova trigger for formation of the solar system (Cameron and Truran, 1977) and with the aerogel-model (Ouellette et al., 2005), whereby short-lived radionuclides from a supernova are injected into an already-formed protoplanetary disk (Chevalier, 2000). To constrain the initial solar system abundance of ^{126}Sn, concentration data for Sn and Te have been acquired for all leachate fractions. These latter results are of additional interest, because they provide new information on the host phases of Sn and Te in carbonaceous chondrites.

2. Samples and experimental procedures

New Te isotope composition data were acquired for sequential digestions of the carbonaceous chondrites Orgueil (CI1), Murchison (CM2, USNM 5459), and Allende (CV3, USNM 6159). For Murchison and Allende, two separately leached powder splits (samples a and b) were analyzed. The same dissolutions were also analyzed for Zr isotopes in a parallel study by Schönbächler et al. (2003, 2005). The chemical and mass spectrometric techniques mainly follow the methods described in Fehr et al. (2004). The most important aspects of the procedures and any modifications introduced for this study are outlined below.

Between 0.8 and 2.0 g of powdered Orgueil, Murchison, and Allende were sequentially treated with acids of increasing strength (Table 1) using a procedure adapted from published methods (Rotaru et al., 1992; Podosek et al., 1997a; Dauphas et al., 2002a). The final dissolution step was performed with conc. HF–HNO_3 in a Teflon bomb with steel jacket, which leaves no visible residues. For Allende-a, a high-pressure asher (Anton Paar, Austria) was used for the final digestion. In this case, the sample was treated with aqua regia in a closed quartz glass vessel, which was placed inside a pressure vessel at 220 °C and filled with nitrogen to a pressure of 130 bar.

A small aliquot (5–15%) of each leach fraction was used for the concentration measurements, whereas the remainder was further processed by column chromatography for the isolation of Te and Zr for isotopic analysis. The separation of these elements utilized two different procedures. For Orgueil, Murchison-a, and Allende-b, a method that was originally developed for the isolation of W and Zr (Schönbächler et al., 2004 and references therein) was used. Tellurium was stripped from the first column with 1 M HNO_3 after the elution of Zr and W. From the leachates of Murchison-b and Allende-a, Te was isolated with the two-stage chromatographic procedure of Fehr et al. (2004). The second separation step of this method, which isolates Te from Sn with Tru-Spec™ resin, was applied to all samples.

The total chemistry blank was <120 pg Te throughout this study. For samples with more than 20 ng Te this contribution is negligible at less than 0.6%. Most samples of leach steps 2–4 (Table 2) had more than 100 ng Te and the Te blank was only 30 pg (0.03%) or lower. For leachates that released less than ~2% of the total Te present in a sample, the blank contribution is enhanced, because the Te recovery was only 0.1–7 ng (leach steps 1 and 5, Table 2). However, only two samples (leach steps 5b of Murchison-b and 1b of Allende-a) have a blank contribution of more than 6%.

The Te isotopic measurements were performed with a Nu Plasma MC-ICPMS at the ETH Zürich using Ni skimmer cones with narrow exit angles (NA-type cones, Nu instruments part # 319 284; Fehr et al., 2004). Most measurements comprised the collection of 80 ratios (5 s integrations) by static multiple collection with Faraday cups, except for samples with low Te contents, for which only 20–60 ratios were acquired. The acetic acid (HAc) leachate of Allende-a, which had the lowest Te recovery of 100 pg, was analyzed using a time-resolved software protocol (which optimizes the time spent on data acquisition) on only 50 µl of sample solution (15–30 s analysis time) and with a total Te ion beam of 6×10^{-13} A. For small amounts of Te, it is advantageous to measure short signals of high intensity instead of performing longer analysis at low ion beam intensities, as the former method provides better precision. Measurements obtained with the time-resolved software consume 4–6 times less Te compared to solutions of the same concentration analyzed with the standard software, whereas the achievable reproducibility is similar for both methods (Fig. 1).

For mass fractionation correction by internal normalization, the measured Te isotope ratios were primarily normalized to ^{125}Te/^{126}Te = 0.374902 (Lee and Halliday, 1995) with the exponential law.

Table 1
Experimental procedure for the leaching of carbonaceous chondrites

Step	Reagent	Procedure	Samples
1a	2.5% HAc	30 min, RT	Murchison-a + b, Orgueil
1b	50% HAc	1 day, RT	All samples
2	4 M HNO_3	5 days, RT	All samples
3a	6 M HCl	5 days, RT	Murchison-b
3b	6 M HCl	1 day, 36 °C	Murchison-b
3c	6 M HCl	1 day, 80 °C	All samples
4	13.5 M HF–3 M HCl	4 days, 100 °C	All samples
5a	conc. aqua regia	3 h, 220 °C, HPA	Allende-a
5b	conc. HF–HNO_3	3 days, 170 °C, steel bomb	Allende-b, Murchison-a + b, Orgueil

RT, room temperature; HAc, CH_3COOH; HPA, high pressure asher.

Table 2
Te isotopic data

Sample	#[a]	ng Te[b]	Blank (%)[c]	$\varepsilon^{120}Te_{56}$	$\varepsilon^{122}Te_{56}$	$\varepsilon^{124}Te_{56}$	$\varepsilon^{126}Te_{58}$	$\varepsilon^{128}Te_{56}$	$\varepsilon^{130}Te_{56}$
Orgueil (CI1)									
Orgueil bulk[d]	8			9 ± 50	−1.2 ± 2.1	−0.6 ± 1.2	−0.2 ± 0.3	0.5 ± 1.0	1.3 ± 2.0
Leach 1a—2.5% HAc	1	1.5	4	1003 ± 5766	107 ± 165	56 ± 86	24 ± 24	−72 ± 73	−130 ± 146
Leach 1b—50% HAc	1	44	0.14	−27 ± 71	−1.8 ± 2.7	−1.9 ± 1.5	−0.1 ± 0.5	0.4 ± 1.4	1.7 ± 2.5
Leach 2—4 M HNO_3	2	114	0.05	13 ± 57	−1.6 ± 2.4	−1.0 ± 1.3	−0.4 ± 0.4	1.3 ± 1.2	3.2 ± 2.2
Leach 3c—6 M HCl 80 °C	5	398	0.02	−5 ± 52	−0.7 ± 2.2	−0.6 ± 1.2	−0.1 ± 0.3	0.3 ± 1.1	0.9 ± 2.0
Leach 4—13.5 M HF + 3 M HCl	1	48	0.13	−66 ± 71	−0.1 ± 2.7	−0.2 ± 1.5	−0.1 ± 0.5	0.4 ± 1.4	0.9 ± 2.5
Leach 5b—HF–HNO_3 bomb	1	7	0.9	−191 ± 589	15 ± 19	4.6 ± 7.3	1.1 ± 3.0	−3.3 ± 9.0	−5 ± 18
Murchison (CM2), USNM 5459									
Murchison bulk[d]	6			−20 ± 51	−0.3 ± 2.2	0 ± 1.2	0.0 ± 0.3	−0.1 ± 1.1	0.3 ± 2.1
Murchison-a									
Leach 1b—50% HAc	1	4	1.5	40 ± 473	−17 ± 37	−13 ± 15	−2.4 ± 5.6	7 ± 17	14 ± 34
Leach 2 - 4 M HNO_3	1	80	0.08	−34 ± 71	−2.3 ± 2.7	−1.5 ± 1.5	−0.4 ± 0.4	1.1 ± 1.4	3.5 ± 2.5
Leach 3c—6 M HCl 80 °C	4	361	0.02	0 ± 54	−1.9 ± 2.2	−1 ± 1.2	−0.3 ± 0.3	0.8 ± 1.1	1.9 ± 2.1
Leach 4—13.5 M HF + 3 M HCl	1	39	0.15	−2 ± 71	−2.9 ± 2.7	−1.7 ± 1.5	−0.1 ± 0.4	0.2 ± 1.4	1.5 ± 2.5
Leach 5b—HF–HNO_3 bomb	1	5	1.2	209 ± 589	1 ± 19	7 ± 7	1.9 ± 3.0	−6 ± 9	−8 ± 18
Murchison-b									
Leach 1a—2.5% HAc	1	1.6	3.8	−1762 ± 7055	−1 ± 265	−36 ± 198	0 ± 38	0 ± 114	3 ± 219
Leach 1b—50% HAc	1	6	1.0	−70 ± 1085	−7 ± 38	−1 ± 19	−1.0 ± 5.1	3 ± 15	5 ± 28
Leach 2—4 M HNO_3	1	76	0.08	7 ± 82	−1.9 ± 2.9	−0.8 ± 1.5	−0.3 ± 0.4	0.9 ± 1.4	1.8 ± 2.7
Leach 3a—6 M HCl cold	4	1410	0.004	13 ± 53	−0.6 ± 2.2	−0.2 ± 1.2	0.0 ± 0.3	0.0 ± 1.1	0.1 ± 2.1
Leach 3b—6 M HCl 36 °C	3	243	0.02	23.9 ± 54.7	−1.1 ± 2.3	−0.6 ± 1.2	−0.2 ± 0.3	0.6 ± 1.1	1.2 ± 2.1
Leach 3c—6 M HCl 80 °C	1	74	0.08	11 ± 82	−0.5 ± 2.9	0.1 ± 1.5	−0.1 ± 0.4	0.4 ± 1.4	0.8 ± 2.7
Leach 4—13.5 M HF + 3 M HCl	1	20	0.3	172 ± 473	7 ± 37	5 ± 15	2.4 ± 5.6	−7 ± 17	−13 ± 34
Leach 5b—HF–HNO_3 bomb	1	0.3	20	534 ± 7055	15 ± 265	−16 ± 198	21 ± 38	−62 ± 114	−94 ± 219
Allende (CV3), USNM 6159									
Allende bulk[e]	17			0 ± 49	−0.6 ± 2.1	−0.3 ± 1.1	0.0 ± 0.3	0.0 ± 1.0	0.4 ± 2.0
Allende bulk bomb[d]	2			24 ± 55	0.7 ± 2.5	−0.1 ± 1.2	0.1 ± 0.4	−0.3 ± 1.3	−0.7 ± 2.5
Allende-a									
Leach 1b—50% HAc[f]	1	0.1	60	1611 ± 7560	−165 ± 164	−144 ± 65	−20 ± 27	60 ± 74	
Leach 2—4 M HNO_3	1	48	0.13	1 ± 55	1.2 ± 2.7	0.3 ± 1.5	0.2 ± 0.8	−0.7 ± 1.4	−0.9 ± 2.7
Leach 3c—6 M HCl 80 °C	4	718	0.008	1 ± 51	−0.9 ± 2.1	−0.1 ± 1.2	−0.1 ± 0.3	0.4 ± 1.1	0.9 ± 2.1
leach 4—13.5 M HF + 3 M HCl	2	295	0.02	41 ± 57	−1.0 ± 2.3	−0.6 ± 1.3	0.0 ± 0.4	0.1 ± 1.2	0.9 ± 2.2
Leach 5a—aqua regia HPA	1	3.2	1.9	37 ± 358	6 ± 21	−1 ± 11	0.5 ± 3.9	−1 ± 12	−2 ± 21
Allende-b									
Leach 1b—50% HAc	1	3.2	1.9	−146 ± 1330	−2 ± 55	−8 ± 37	−3 ± 8	8 ± 25	19 ± 49
Leach 2—4 M HNO_3	1	89	0.07	−38 ± 65	−0.3 ± 2.8	−0.6 ± 1.4	0.1 ± 0.4	−0.4 ± 1.4	0.4 ± 2.6
Leach 3c—6 M HCl 80 °C	2	174	0.03	−2 ± 60	−2.2 ± 2.6	−1.4 ± 1.4	−0.4 ± 0.4	1.3 ± 1.3	2.9 ± 2.5
Leach 4—13.5 M HF + 3 M HCl	1	60	0.10	−17 ± 71	−2.6 ± 2.7	−1.6 ± 1.5	−0.3 ± 0.5	0.9 ± 1.4	2.6 ± 2.5
Leach 5b—HF–HNO_3 bomb	1	1.1	5.5	−3992 ± 4094	−50 ± 175	−56 ± 75	−7 ± 13	20 ± 33	56 ± 70
Synthetic samples (doped with Te standard)									
Iron-meteorite matrix [e]	6			−1 ± 50	−1.2 ± 2.1	−0.5 ± 1.1	−0.1 ± 0.3	0.3 ± 1.0	0.8 ± 2.0
Chondrite matrix [e]	7			0 ± 49	−0.7 ± 2.1	−0.3 ± 1.1	−0.1 ± 0.3	0.2 ± 1.0	0.8 ± 2.0
Diorite matrix[e,g]	15			−9 ± 51	−1.0 ± 2.2	−0.9 ± 1.1	−0.2 ± 0.3	0.5 ± 1.1	1.5 ± 2.0
Diorite matrix, W-Zr method[e,h]	4						−0.1 ± 0.3	0.3 ± 1.5	0.8 ± 2.4
Synthetic spectra[i]									
p-process excess				100	0.0	0.0	0.0	0.0	0.0
r-process excess Richter[j]				0	0.0	0.0	−1.7	5.0	4.9
r-process excess Maas[k]				0	0.0	0.0	−1.7	5.0	12
r-process excess Meyer[l]				−7	−5.0	−2.5	−1.4	4.0	11
s-process excess[m]				6	9.0	6.2	1.9	−5.6	−8.3
s-process depletion[m]				−6	−9.0	−6.2	−1.9	5.6	8.3

Combined mean values are shown for samples with multiple analyses. The quoted analytical uncertainties (2σ) include the errors for standard and sample measurements and for the blank. The error from the blank was calculated assuming an uncertainty of 100% for the blank and a difference in the isotope composition of 1‰. The blank contributes a significant fraction (~3%) to the $\varepsilon^{126}Te$ uncertainty of leach 1b for Allende-a; for all other results the additional uncertainty from the blank correction is <1%. HAc, CH_3COOH; HPA, high pressure asher.

$\varepsilon^{x}Te_{56} = \{[(^{x}Te/^{125}Te)_{sample} - (^{x}Te/^{125}Te)_{std}]/(^{x}Te/^{125}Te)_{std}\} \times 10^4$, normalized to $^{125}Te/^{126}Te = 0.374902$ (Lee and Halliday, 1995) with the exponential law;

$\varepsilon^{126}Te_{58} = \{[(^{126}Te/^{128}Te)_{sample} - (^{126}Te/^{128}Te)_{std}]/(^{126}Te/^{128}Te)_{std}\} \times 10^4$, normalized to $^{125}Te/^{128}Te = 0.22204$ (Lee and Halliday, 1995) with the exponential law;

(*continued on next page*)

Table 2 (*continued*)

[a] # denotes the number of individual measurements.
[b] Recovered amount after chemical separation.
[c] Blank contribution was calculated assuming a blank of 60 pg Te.
[d] From Fehr et al. (2005).
[e] From Fehr et al. (2004).
[f] No ε^{130}Te values are shown because of a known Ba interference.
[g] Eight individual measurements for ε^{120}Te and ε^{122}Te, 2 measurements for ε^{130}Te.
[h] No ε^{120}Te, ε^{122}Te and ε^{124}Te values are shown because of known Sn interferences.
[i] Synthetic spectra are calculated assuming *r*-process compositions as measured by Richter et al. (1998)[j] and Maas et al. (2001)[k] and as calculated by Meyer in Maas et al. (2001)[l]; *s*-process compositions are from Arlandini et al. (1999)[m].

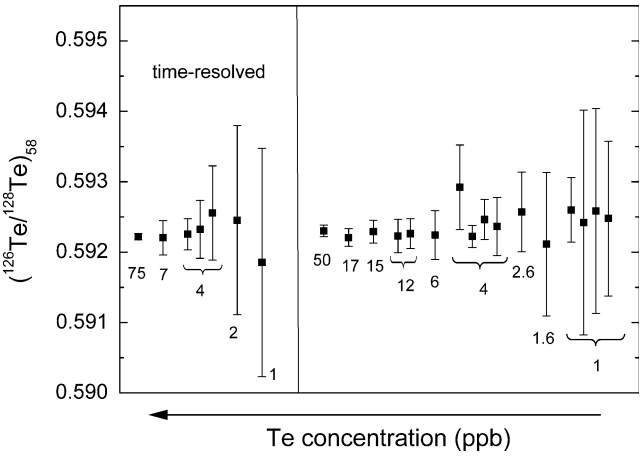

Fig. 1. Isotopic results for Te standard solutions with concentrations of 1–75 ppb. Each data point represents the mean of 6–30 individual measurements. The quoted errors are 2σ external reproducibilities. The $(^{126}Te/^{128}Te)_{58}$ ratios were determined using Faraday collectors with and without use of the time-resolved software and are internally normalized relative to $^{125}Te/^{128}Te$. The numbers denote the concentration of the Te standard in ppb. Measurements obtained with the time-resolved software consume 4–6 times less Te compared to solutions of the same concentration analyzed with the standard software.

The $\varepsilon^{x}Te_{56}$ values (whereby the subscript denotes the normalization method) of the samples were then calculated relative to the mean isotopic data obtained for a JMC Te standard on the same day using $\varepsilon^{x}Te_{56} = \{[(^{x}Te/^{125}Te)_{sample} - (^{x}Te/^{125}Te)_{std}]/(^{x}Te/^{125}Te)_{std}\} \times 10^4$. Additionally, $^{126}Te/^{128}Te$ isotope ratios were normalized with the exponential law relative to $^{125}Te/^{128}Te = 0.22204$ (Lee and Halliday, 1995) and are reported as $\varepsilon^{126}Te_{58}$.

For 100–150 ppb Te standard solutions, the reproducibility (2σ) on one day is typically $\pm 47\ \varepsilon$ for $^{120}Te/^{125}Te$, $\pm 2.0\ \varepsilon$ for $^{122}Te/^{125}Te$, $\pm 1.1\ \varepsilon$ for $^{124}Te/^{125}Te$, $\pm 1.0\ \varepsilon$ for $^{128}Te/^{125}Te$, $\pm 1.9\ \varepsilon$ for $^{130}Te/^{125}Te$ (all previous ratios are normalized to $^{125}Te/^{126}Te$), and $\pm 0.3\ \varepsilon$ for $(^{126}Te/^{128}Te)_{58}$. If less than 100 ng Te is analyzed, the error on the isotopic composition is larger, however. Tellurium isotope measurements for standard solutions with Te concentrations of 1–50 ppb were performed on seven measurement sessions over a period of about 9 months. The $^{x}Te/^{128}Te$ ratios remained constant with time and showed no dependence on concentration. The results for $(^{126}Te/^{128}Te)_{58}$, in the form of mean values obtained for 6–30 individual measurements, are shown in Fig. 1. Similar analyses were performed using the time-resolved approach on three measurement sessions (Fig. 1). The reproducibility of 17 Allende chondrite measurements is similar to the reproducibility obtained for repeated analyses of the Te standard (Fehr et al., 2004). Therefore, the reproducibility (2σ) of isotopic measurements for Te standard solutions with matching concentrations was used as a conservative estimate for the 2σ uncertainties of both the standard and sample measurements. For the calculation of mean values, the variances from duplicates were combined quadratically assuming a single population. The uncertainty that is introduced by the blank (Table 2) was estimated by assuming a mean blank of 60 ± 60 pg, and a difference in the Te isotope composition of 1‰. Based on this, the blank contribution is responsible for less than 3% of the total uncertainty of the Te isotope data.

The Sn and Te abundances of the samples were measured by quadrupole ICP-MS on sample solution aliquots that did not undergo chemical separation to avoid any chemical fractionation of Sn from Te. Concentrations were determined after an external calibration that utilized synthetic standard solutions. Samples and standards were prepared in 0.5 M HNO_3 and 0.01 M HF to stabilize Sn and Te and prevent precipitation of SnO_2. Rhodium, Cd, and Sm were used as internal standards to compensate for non-spectral interferences. A blank correction was performed by subtracting the ion beam intensities obtained for the blank from those of the corresponding samples. The analyses typically have a precision of better than 10% relative standard deviation (2σ) for concentrations above 0.5 μg/l Sn and Te. The limits of detection (LODs) were 0.01 μg/l for ^{118}Sn and 0.05 μg/l for ^{128}Te, corresponding to about 0.1–5 ppb (ng/g) Sn and 0.5–25 ppb Te in the original samples, depending on the final dilution. The reproducibility of the Sn, Te, and Sn/Te data is about ±20%, based on repeated measurements of bulk Allende and accounting for minor material loss during the leaching procedure. The uncertainties of the individual sample and blank measurements were added to the 20% uncertainty, but this contribution is negligible for sample solutions above 0.5 μg/l Sn and Te. For Sn and Te concentrations close to the LOD, the total uncertainties are larger but for most samples they are still better than about 30% (Table 3).

The Mg, Na, K, and Ca concentrations of the Orgueil leach fractions (Table 4) were also determined by quadrupole ICP-MS on separate solution aliquots using techniques similar to those applied for Sn and Te. It is evident that the total combined K and Ca abundances of the leachates are significantly lower than published results for bulk samples of Orgueil (Table 4), and this difference can be only partly explained by the material loss that occurred during the leaching procedure. The discrepancy probably reflects that these concentration data are essentially by-products of multi-element analyses that focused primarily on high-mass (>80 amu) elements. Regardless of this shortcoming, the data are nonetheless suitable for evaluating the relative abundances of the respective elements in the various leachate fractions.

3. Results and discussion

3.1. Distribution of Sn and Te in the leachates—implications for their host phases

Tin and Te are both moderately volatile elements with half mass condensation temperatures of 703 and 705 K, respectively, and they are thought to condense primarily as alloys with Fe at total gas pressures of 10^{-4} bar (Lodders, 2003). Due to this similarity in behavior, Sn/Te ratios are unlikely to be fractionated significantly during condensation in the early solar nebular and any larger fractiona-

Table 3
Distribution of Sn and Te in leachates of carbonaceous chondrites

	Sn (ppb) rel. to bulk[a]	Te (ppb) rel. to bulk[a]	Sn (ppb)[b]	Te (ppb)[b]	$^{124}Sn/^{128}Te$
Orgueil: 1.0 g					
1a—2.5% HAc	0.7 ± 0.2	2.0 ± 0.5	18	50	0.07 ± 0.02
1b—50% HAc	1.3 ± 0.3	109 ± 22	8	663	0.0022 ± 0.0005
2—4 M HNO_3	196 ± 40	1,101 ± 223	190	1,063	0.033 ± 0.007
3c—6 M HCl 80 °C	504 ± 102	874 ± 180	1,154	2,001	0.11 ± 0.02
4—13.5 M HF–3 M HCl	155 ± 31	99 ± 20	8,055	5,139	0.29 ± 0.06
Total Orgueil	858	2,185			
Bulk Orgueil[c]	1,150	2,490			
Murchison-a: 1.5 g					
1a—2.5% HAc	0.6 ± 0.1	2.9 ± 0.7	28	138	0.036 ± 0.011
1b—50% HAc	6 ± 1	22 ± 5	26	104	0.045 ± 0.011
2—4 M HNO_3	71 ± 16	784 ± 155	54	595	0.016 ± 0.004
3c—6 M HCl 80 °C	631 ± 126	444 ± 89	3,184	2,238	0.26 ± 0.05
4—13.5 M HF–3 M HCl	158 ± 31	64 ± 13	30,004	12,177	0.45 ± 0.09
Total Murchison-a	867	1,317			
Murchison-b: 2.0 g					
1a—2.5% HAc	0.8 ± 0.2	1.6 ± 0.4	51	108	0.09 ± 0.03
1b—50% HAc	2.4 ± 0.5	8 ± 2	12	41	0.055 ± 0.014
2—4 M HNO_3	35 ± 7	371 ± 75	25	264	0.017 ± 0.004
3a—6 M HCl cold	559 ± 114	785 ± 158	2,400	3,368	0.13 ± 0.03
3b—6 M HCl 36 °C	99 ± 19	135 ± 28	2,467	3,360	0.13 ± 0.03
3c—6 M HCl 80 °C	23 ± 5	32 ± 7	978	1,340	0.13 ± 0.03
4—13.5 M HF–3 M HCl	85 ± 17	11 ± 3	3,641	473	1.39 ± 0.33
5b—HF–HNO_3, bomb	7 ± 2	6 ± 2	335	296	0.21 ± 0.05
Total Murchison-b	812	1,350			
Bulk Murchison[c]	720	1,660			
Allende-a: 2.0 g					
1b—50% HAc	7 ± 1	1.1 ± 0.6	21	3	1.17 ± 0.62
2—4 M HNO_3	7 ± 3	172 ± 39	5	132	0.007 ± 0.003
3c—6 M HCl 80 °C	195 ± 40	539 ± 116	576	1,594	0.067 ± 0.014
4—13.5 M HF–3 M HCl	255 ± 50	216 ± 44	2,409	2,044	0.22 ± 0.04
5a—aqua regia, HPA	3 ± 3	18 ± 6	13	71	0.03 ± 0.03
Total Allende-a	466	946			
Bulk Allende[c]	543	1,034			

HAc, CH_3COOH; HPA, high pressure asher.
[a] Elemental concentrations calculated relative to the weight of the bulk sample.
[b] Concentrations relative to dissolved mass. The uncertainties of the data are difficult to estimate due to the uncertainty of the actual dissolved mass, which was approximated by the weight of the dried leach solution.
[c] From Fehr et al. (2005).

Table 4
Mg, Na, K, and Ca concentrations of the Orgueil leach fractions

Orgueil leach steps	Mg (%)	Na (ppm)	K (ppm)	Ca (ppm)
1a—2.5% HAc	0.3	>728	88	1217
1b—50% HAc	0.5	1704	82	<5
2—4 M HNO_3	5.6	320	77	<39
3c—6 M HCl 80 °C	0.6	36	6	<13
4—13.5 M HF–3 M HCl	0.1	4	1	<1
Total Orgueil	7.1	>2791	254	1217
Bulk Orgueil[a]	9.6	4990	543	9076

Elemental concentrations are calculated relative to the weight of the bulk sample. HAc, CH_3COOH.
[a] From Lodders (2003).

tions should thus reflect later processes. For example, any subsequent sulfurization of Fe-alloys may be associated with a redistribution of Te from the metal phase into troilite, due to the strong chalcophile affinity of this element. Direct condensation of Te into troilite is also possible but this occurs primarily at lower gas pressures of 10^{-6} bar with a 50% condensation temperature of 694 K (Lodders, 2003). In the following, the observed distribution patterns of Sn and Te in the different acid leachates of Orgueil, Murchison, and Allende (Fig. 2, Table 3) are evaluated, as they provide new constraints on the host phases of these elements in carbonaceous chondrites. The Sn and Te abundances are reported as elemental concentrations in the

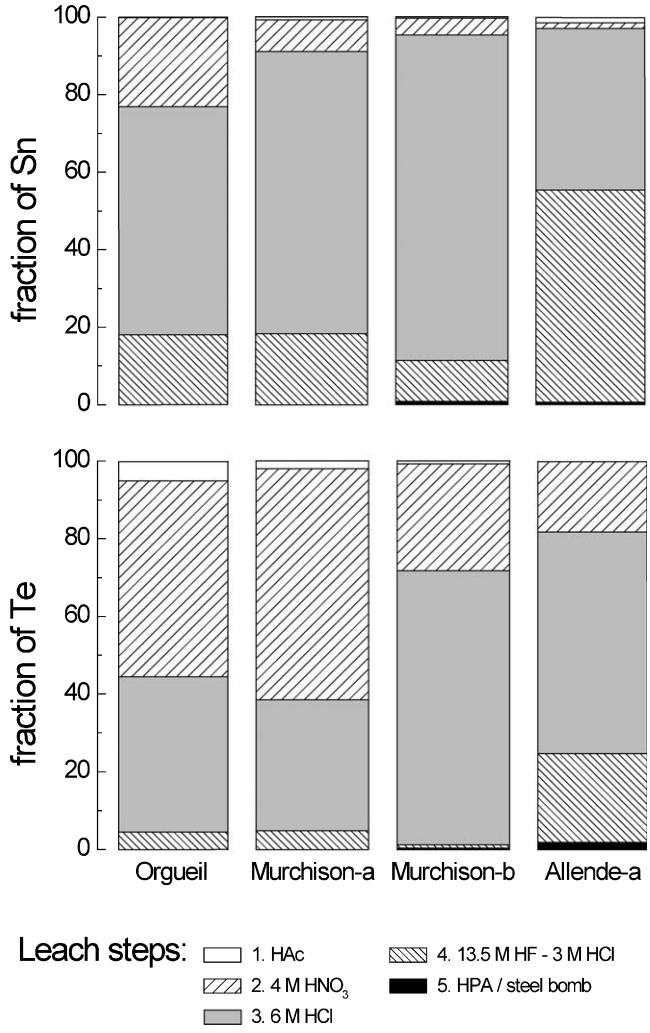

Fig. 2. Distribution of Sn and Te in sequentially leached bulk rock powders of Orgueil, Murchison, and Allende. Data are from Table 3. HAc, CH_3COOH; HPA, high pressure asher.

whole rock (relative to the initial bulk sample) and as concentrations relative to the dissolved mass of each leachate fraction (as calculated from the mass of the dried leach solution). The latter values are a measure of the actual Sn and Te concentrations of the material that was dissolved in a particular leaching step.

Most of the Sn (60–84%) was released in the 6 M HCl leachates except for Allende-a, where the majority of the Sn was present in the 13.5 M HF–3 M HCl leachate (55%) and slightly less (42%) in the 6 M HCl fraction. Only minor amounts of Sn (<2%) were released by acetic acid (HAc) and during the final dissolution step. Tellurium shows a slightly different release pattern. Most of the Te was present in the 4 M HNO_3 and the 6 M HCl leachates (75–98%). For Murchison-b, three subsequent 6 M HCl leach steps were performed at different temperatures. During this experiment, the majority of both the Sn and Te were released by 6 M HCl at room temperature (60–70%), whereas the following HCl steps revealed significantly lower Sn and Te contents with 10–12% and 2–3% of the total Sn and Te, respectively. For Orgueil, a significant fraction (5%) of the total Te was already leached from the sample with 50% HAc. The HAc leachates of the other meteorites and all final digestion steps contained less than 2% of the total Te budgets.

Tellurium is strongly chalcophile, but it can also behave as a siderophile element if sulfides are not present (Mason and Graham, 1970; Leutwein, 1972; Allen and Mason, 1973; Lodders, 2003). In this study, the majority of the Te was present in leach steps 2 (HNO_3), 3 (HCl), and 4 (HF–HCl; Table 3, Fig. 2). It is therefore possible that this distribution reflects the partial leaching of sulfides by HNO_3 and subsequent further dissolution by HCl. However, it is also conceivable that the Te release patterns are due to the presence of distinct sulfide phases that are preferentially attacked by acids of different strength. As the analyzed meteorites contain only minor amounts of metal, the distribution of Te in the leachates is in accord with the conclusion that sulfides are important carrier phases of this element in carbonaceous chondrites.

Previous heating experiments on ordinary and carbonaceous chondrites indicate that Te is hosted in two main phases in these meteorites, most probably troilite and an additional low-temperature phase (Ikramuddin et al., 1977; Matza and Lipschutz, 1977; Lauretta et al., 2002) that appears to be soluble in hot water (Goles and Anders, 1962; Reed and Allen, 1966). Goles and Anders (1962) suggested that this water-soluble mineral could be epsomite ($MgSO_4$) for the carbonaceous chondrite Murray. Reed and Allen (1966) reported that 63% of the Te in Orgueil is leachable with hot water. This indicates that sulfates may host significant quantities of tellurium. Several lines of evidence, however, argue against the interpretation that sulfates are an important carrier phase of Te in carbonaceous chondrites and their parent bodies. First, the sulfates of Orgueil are thought by some to be primarily of terrestrial origin (formed by reaction with atmospheric water and/or oxidation processes that occurred during sample storage) and not a primary feature of the meteorites (Gounelle and Zolensky, 2001). Second, it has been shown that only Orgueil has abundant sulfate, whereas sulfates are rare in Murchison and absent in Allende (Burgess et al., 1985, 1991). Third, for all three carbonaceous chondrites, only minor amounts of Te (<5%) were released with HAc in the first stage of the leaching process (Table 3, Fig. 2). In contrast, Fredriksson and Kerridge (1988) showed that the water-soluble phases of Orgueil contain virtually the complete Na and K budget, as well as about 50% of the Ca and 11% of the Mg. Based on this, they concluded that sulfates and carbonates had been dissolved. In this study, the complete Ca inventory, more than 87% of the Na and 67% of all K were released by leaching of Orgueil with HAc. This suggests that those phases that are leachable with hot water in Orgueil were also digested by the HAc leach steps of our procedure. The absence of significant quantities of Te in the HAc leachates of Orgueil thus implies that only a very minor part of the Te of this meteorite

is hosted in sulfates. By inference, this conclusion also applies to Murchison and Allende. The reason for the discrepancy between the data of the present study and the results of Reed and Allen (1966) is unclear at present, but it may reflect primary sample heterogeneity, heterogeneities in the distribution of altered phases or, alternatively, analytical artifacts.

Tin is mainly siderophile with some chalcophile and lithophile affinities (Hamaguchi and Kuroda, 1969; Buseck, 1970; Mason and Graham, 1970; Allen and Mason, 1973). The analyzed carbonaceous chondrites contain only minor amounts of metal and the distribution of Sn and Te in the leachates is similar (Fig. 2, Table 3). This implies that sulfides, which are thought to be the main carrier of Te, could also be an important host phase for Sn in carbonaceous chondrites. Such a conclusion stands in contrast to the occurrence of Sn in iron meteorites and ordinary chondrites, where it is mainly present in the metal phase (Shima, 1964; Mason and Graham, 1970; Fehr et al., 2005). However, as the carbonaceous chondrites analyzed in this study contain less than 0.5% metal, Sn may display the same chalcophile affinity that has been documented for its occurrence in the Earth's crust, where it is often enriched in sulfides (Yi et al., 1995).

Magnetite and ilmenite are the two phases that display the largest enrichments of Sn in the terrestrial mantle (Noll et al., 1996). Furthermore, Sn can be found as Sn-oxide in chondritic interplanetary dust particles (Rietmeijer, 1989). This suggests that oxides could also be an important host phase for Sn in meteorites, particularly given that the carbonaceous chondrite Orgueil consists of about 10% magnetite (Hyman et al., 1979; Hyman and Rowe, 1983). In general, oxides should not dissolve in HNO_3 but they may be leached by HCl (Johnson and Maxwell, 1981). In the present study, the HCl fraction contains most of the Sn released from Orgueil. Magnetite may, therefore, be the host for some of the Sn released in that step. However, the magnetite of CI chondrites has extremely low concentrations of minor elements (Brearley and Jones, 1998). In addition, similar amounts of Sn were leached by HCl from Murchison, Allende, and Orgueil (Table 3, Fig. 2), even though the former meteorites have only minor magnetite contents. This suggests that magnetite cannot be a main carrier phase of Sn in the investigated meteorites.

The presence of significant amounts of Sn (11–55%) and Te (1–23%) in the HF–HCl leachates, furthermore, implies that some silicate phases may be enriched in these elements, such that they carry a significant part of the elemental budgets (Table 3, Fig. 2). This is particularly true for Sn, which is known to be concentrated in minerals such as feldspar, amphibole, biotite and titanite in terrestrial rocks (Hamaguchi and Kuroda, 1969). Alternatively, the release of Te and Sn by HF–HCl leaching may reflect, at least in part, the digestion of small sulfide and metal inclusions within silicates that were previously shielded from dissolution by HNO_3 and HCl.

3.2. Variations in $^{126}Te/^{128}Te$ and the initial $^{126}Sn/^{124}Sn$ of the solar system

The leaching procedure (Table 1) offers the potential to attack phases of carbonaceous chondrites, which formed very early in the solar system and that are characterized by different Sn/Te ratios. Such leachates may thus exhibit variations in the relative abundance of ^{126}Te from the decay of formerly live ^{126}Sn. Although the overall distribution of Sn and Te in the various leach fractions is similar (Fig. 2), the $^{124}Sn/^{128}Te$ ratios of the leachates vary considerably, from about 0.002 to 1.4 (Table 3). Despite this range in Sn/Te, the leachates of Orgueil, Murchison, and Allende reveal no variability in the relative abundance of ^{126}Te and all have $\varepsilon^{126}Te$ values that are identical to the terrestrial standard and bulk carbonaceous chondrites within the analytical precision (Table 2).

In order to constrain the initial solar system abundance of ^{126}Sn, the $(^{126}Te/^{128}Te)_{58}$ data are plotted in isochron diagrams as a function of $^{124}Sn/^{128}Te$ (Fig. 3). The slopes of the regression lines in these diagrams define an initial $^{126}Sn/^{124}Sn$ of $<31\times10^{-5}$ for Orgueil, of $<9.4\times10^{-5}$ for Murchison, and of $<16\times10^{-5}$ for Allende. If all the leachate data are combined (Fig. 3d), the slope indicates an initial $^{126}Sn/^{124}Sn$ of $<7.7\times10^{-5}$ at the time of closure of the Sn–Te system in the carrier phases. Based on results obtained for bulk carbonaceous chondrites, Fehr et al. (2005) deduced an initial solar system $^{126}Sn/^{124}Sn$ ratio of $<18\times10^{-5}$, which overlaps with the more restrictive values calculated from the new data. Please note that the initial abundance of ^{126}Sn was reported as $^{126}Sn/^{118}Sn$ in Fehr et al. (2005). The stable nuclide ^{124}Sn is more useful for normalization than ^{118}Sn, however, because both ^{124}Sn and ^{126}Sn are pure *r*-process isotopes, whereas ^{118}Sn is produced mainly by the *s*-process (Arlandini et al., 1999).

Given the short half-life of ^{126}Sn, it is essential to realize that the lack of resolvable effects for $^{126}Te/^{128}Te$ merely provides evidence that the level of ^{126}Sn was too low to be detectable in the analyzed samples and this limits the amount that could have been present in the early solar system. In this respect, it is also important to consider the following issues:

(1) The leachates display a much larger range of $^{124}Sn/^{128}Te$ ratios than bulk samples of carbonaceous chondrites ($^{124}Sn/^{128}Te \approx 0.07$–$0.24$; Fehr et al., 2005) but they do not exhibit the very high parent–daughter ratios that have aided the utilization of other short-lived decay systems (e.g., ^{26}Al–^{26}Mg, ^{107}Pd–^{107}Ag). The limited Sn–Te fractionation restricts the amount of formerly live ^{126}Sn that can be detected, in spite of the extremely precise measurement techniques.
(2) It is possible that the lack of radiogenic Te isotope anomalies in bulk carbonaceous chondrites and their leachates reflects redistribution of Te (and/or Sn) by alteration processes, because both elements appear

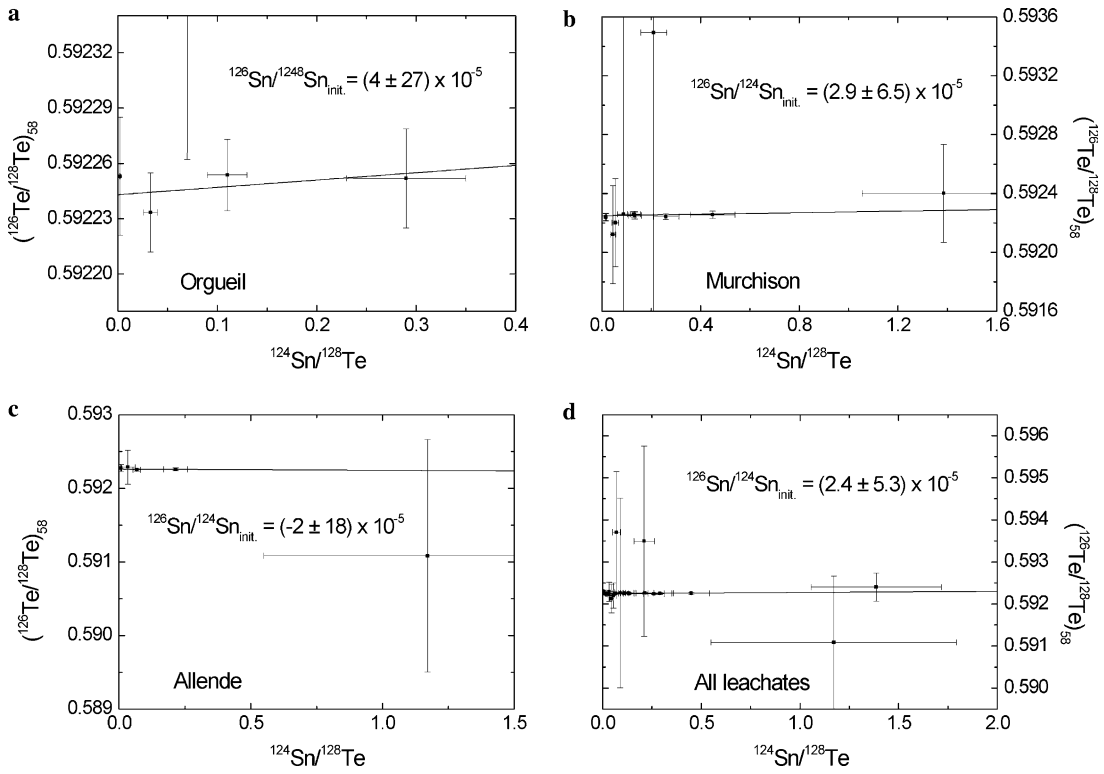

Fig. 3. Sn–Te isochron diagrams for leachates of (a) Orgueil, (b) Murchison, and (c) Allende. In panel (d) all leachate data are combined. The $(^{126}Te/^{128}Te)_{58}$ ratios are the combined mean values of several individual measurements. They are internally normalized relative to $^{125}Te/^{128}Te$ and recalculated from Table 2, assuming $\varepsilon^{126}Te_{58} = 0$ corresponds to $^{126}Te/^{128}Te = 0.592260$ (Fehr et al., 2004). Error bars (2σ) for $(^{126}Te/^{128}Te)_{58}$ represent the combined uncertainties of the sample and standard measurements; the errors for $^{124}Sn/^{128}Te$ are 2σ. The quoted uncertainties for the initial $^{126}Sn/^{124}Sn$ ratios represent the 95% confidence interval.

to be mainly hosted in sulfide phases. Sulfides are readily affected by both thermal metamorphism, which is primarily an issue for Allende, and aqueous alteration, which has been particularly severe for Orgueil and, to a lesser extent, Murchison. It is conceivable that the combined effects of these processes may have compromised the primary sulfide-hosted Te isotope signatures of carbonaceous chondrites (Matza and Lipschutz, 1978; Zolensky and McSween, 1988; Bourot-Denise et al., 1997; Lauretta et al., 1997a; Zanda et al., 1997; Grossman, 2002; Bullock et al., 2005). However, it has also been proposed that at least some sulfides of carbonaceous chondrites are primary unaltered nebular condensates (Lauretta et al., 1997b), and such sulfides would be ideally suited for characterizing the initial solar system abundance of ^{126}Te. A recent study, furthermore, provided evidence for the former presence of the short-lived nuclide ^{36}Cl (half-life 0.3 Myr) in alteration phases of calcium–aluminum-rich inclusions (Lin et al., 2005). Hence, it is unclear to which extent aqueous alteration reflects early nebular processes (that may have occurred while ^{126}Sn was still alive) or reactions that took place primarily on meteorite parent bodies, such that they would have erased any small-scale variations in $^{126}Te/^{128}Te$ (e.g., Zolensky and McSween, 1988; Bischoff, 1998; Brearley, 2004).

(3) It is also possible that anomalies in $^{126}Te/^{128}Te$ were not observed because too little or no ^{126}Sn was synthesized. A type-II supernova can generate a fresh supply of short-lived radioisotopes such as ^{26}Al, ^{41}Ca, ^{53}Mn, ^{60}Fe, and ^{107}Pd, even though very special conditions may be required to obtain initial abundances that are deduced from the published analytical data (Russell et al., 2001; Busso et al., 2003). Such a scenario is able to provide live ^{126}Sn depending on the free decay interval between nucleosynthetic production and the condensation of the first solids. The free decay interval was short enough for ^{126}Sn to be present, if the ^{41}Ca (half-life ~0.103 Myr) and ^{36}Cl that have been detected in meteorites were indeed mainly derived from the same supernova source. So far no supernova models have been published that predict the nucleosynthetic production yields of various isotopes relative to ^{126}Sn. However, the $^{126}Sn/^{124}Sn$ production ratio can be estimated following the method discussed in Meyer and Clayton (2000). The $^{126}Sn/^{124}Sn$ r-process production ratio has to be close to the $^{126}Te(r)/^{124}Sn$ solar system ratio, which is 2.4. Assuming a delay of 1 Myr before the injection of the supernova ejecta (Meyer et al.,

2004), this corresponds to an initial ratio of 0.13 at the time of solar system formation. The application of dilution factors calculated from the observed initial abundances of ^{53}Mn and ^{182}Hf yields initial ^{126}Sn/^{124}Sn ratios of 1.2×10^{-5} and 3.7×10^{-5}, respectively. The constraint of ^{126}Sn/^{124}Sn $<7.7 \times 10^{-5}$, as deduced from the present leachate data (Fig. 3d), can therefore not be used to argue against a supernova trigger for the formation of the solar system or the injection of short-lived radionuclides into an already-formed protoplanetary disk. However, the above calculations demonstrate that the present analytical techniques are precise enough to potentially detect formerly live ^{126}Sn, if phases with highly fractionated Sn/Te ratios could be analyzed.

3.3. Nucleosynthetic Te isotope anomalies

3.3.1. Tellurium isotope compositions of the leachates

The ε^{120}Te, ε^{122}Te, ε^{124}Te, ε^{128}Te, and ε^{130}Te data obtained for the Orgueil, Murchison, and Allende leachates are summarized in Fig. 4 and Table 2. Most samples display small positive ε^{130}Te$_{56}$ and ε^{128}Te$_{56}$ values, whereas they have small negative values for ε^{122}Te$_{56}$ and ε^{124}Te$_{56}$. Nonetheless, the overwhelming majority of the leachates display Te isotope compositions that are identical to the terrestrial standard (ε^{x}Te = 0) within the analytical precision. The HNO_3 fraction of Murchison-a has the most positive ε^{130}Te$_{56}$ of $+3.5 \pm 2.5$ but unfortunately there was only sufficient Te for a single precise measurement. In contrast, the same leach step of Murchison-b does not exhibit a ^{130}Te anomaly as it is characterized by a ε^{130}Te$_{56}$ of $+1.8 \pm 2.7$. This discrepancy may be due to sample heterogeneity, small differences in the leaching procedures, or analytical artifacts. The latter possibility is further discussed below.

3.3.2. Potential analytical problems

Tests conducted with a diorite, a chondrite and an iron-meteorite matrix that were doped with the ε^{x}Te = 0 standard yielded slightly positive ε^{130}Te and negative ε^{122}Te and ε^{124}Te results, which are within uncertainties identical to the pure Te standard (Fehr et al., 2004; Fig. 4 and Table 2). This implies that there are small residual analytical artifacts, which result in enhanced ε^{130}Te and reduced ε^{122}Te, ε^{124}Te values, even though these effects are not fully resolvable given the present uncertainties. It is conceivable that this is due to some residual isotope fractionation effects, as ^{125}Te/^{126}Te is used for fractionation correction.

Matrix tests with a diorite were also performed using the column chemistry procedure that was originally developed for the separation of W and Zr (Fehr et al., 2004). The ε^{120}Te, ε^{122}Te, and ε^{124}Te were not measured, since interfering Sn was not separated by a second column chemis-

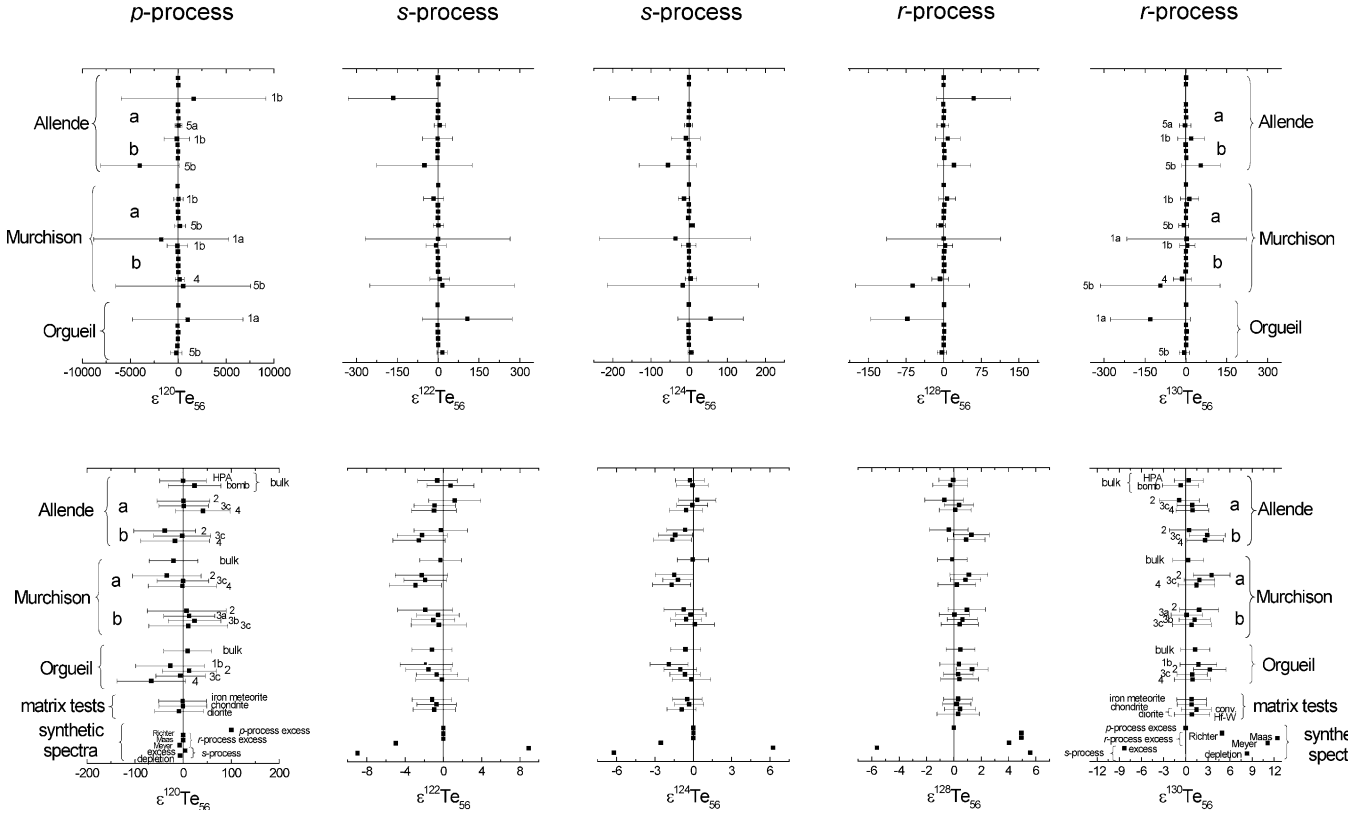

Fig. 4. Results obtained for ε^{120}Te$_{56}$, ε^{122}Te$_{56}$, ε^{124}Te$_{56}$, ε^{128}Te$_{56}$, and ε^{130}Te$_{56}$ for leachates of Orgueil, Murchison, and Allende. The numbers denote the individual leach steps as described in Table 1. Shown are the combined mean values of several measurements. The error bars (2σ) denote the combined uncertainty of the sample and standard measurements. The plots in the top row display all data, whereas the bottom row shows only results obtained at high precision (note the difference in scale). On the top of the first row, the nucleosynthetic processes by which each Te isotope can be formed are shown. The ε^{x}Te$_{56}$ values are calculated with ^{125}Te (produced by the *s*- and *r*-process) as the reference isotope in the numerator of all ratios.

try. The test samples yielded slightly less extreme values of $\varepsilon^{126}Te_{58} = 0.1 \pm 0.3$ and $\varepsilon^{130}Te_{56} = 0.8 \pm 2.4$ than the diorite matrix samples, which were processed using the dedicated Te separation protocol (Table 2, Fig. 4). Therefore, the two separation methods should give identical results. In this respect it is interesting to note that the leachates (Orgueil, Murchison-a, and Allende-b), from which Te was isolated with the W and Zr method, deviate slightly more from $\varepsilon^{x}Te = 0$ than the samples that were treated with the Te separation method of Fehr et al. (2004). This difference is thus unlikely to be the result of the two chemical separation methods.

In the following, various potential analytical problems are evaluated in detail, to assess whether the small observed deviations from $\varepsilon^{130}Te = 0$ for some leachates (Table 2, Fig. 4) indeed reflect real isotopic variations. The evaluation focuses in particular on the HNO_3 leachate of Murchison-a, because this sample displays the largest Te isotope anomaly detected so far for any sample, including the bulk chondrites, iron meteorites and sulfides analyzed in a previous study (Fehr et al., 2005).

The total chemistry yield of the Te separation is typically about 70–80%. However, the use of HNO_3 for sample preparation can significantly reduce the Te yields (Fehr et al., 2004). All HNO_3-leachates of this study, as well as the final dissolutions (step 5, Table 1), had yields of only about 10–15%. This is probably due to the presence of Te in unfavorable complexes and/or an unfavorable oxidation state during loading of the ion-exchange columns. In order to ensure that all Te is available as Te(IV), which is desired, it is essential to treat the samples with conc. HCl prior to the ion-exchange chemistry (Hanson et al., 1957). It is conceivable that these low yields generated mass-dependent Te isotope fractionations that were not adequately corrected for by internal normalization. The analytical data, however, do not provide support for this interpretation. In particular, the HNO_3-leachate of Murchison-a was found to be unfractionated in its stable isotope composition relative to the terrestrial Te standard in $^{126}Te/^{128}Te$, within an analytical uncertainty of about $\pm 0.8‰$, as determined by a standard-sample bracketing technique (Fehr et al., 2005). These uncertainties are, however, an order of magnitude larger than those of the internally normalized Te isotope data.

Spectral interferences from isobars and molecular ions are the most likely alternative sources of analytical artifacts. Both Xe and Ba have isotopes that are isobars of ^{130}Te. For ^{130}Xe, an interference correction was applied online during the measurements. Such a correction was not performed for ^{130}Ba due to the limited number of Faraday cups available for static multiple collection (Fehr et al., 2004). The Ba/Te ratio of each sample was, however, checked prior to the isotopic analyses and only samples with $Ba/Te \leqslant 7.5 \times 10^{-3}$ were analyzed. At this level, the contribution of ^{130}Ba to the ^{130}Te ion beam is insignificant (given the analytical precision) at less than 25 ppm (Fehr et al., 2004).

There are a number of potentially problematic molecular ions, such as SnN, SnO, CdN, CdO, ZrAr, $CrAr_2$, VAr_2, $TiAr_2$, MoO_2 and the sample solutions also contained significant amounts of Al, Ca, Fe, Cu, and Zn. To investigate the effects of these elements, a Te standard solution was doped with known amounts of potentially problematic elements to obtain similar or larger contaminant/Te ratios as those of the sample solutions. The impact of each contaminant element was checked separately as well as in combination with all other elements. These tests were performed in particular for contaminant levels similar to those observed for the HNO_3-leachate of Murchison-a. All doped Te standards had $\varepsilon^{130}Te$ values identical to those of the pure Te standard. Therefore, it is unlikely that the $\varepsilon^{130}Te$ data are biased by spectral interferences or matrix effects.

3.3.3. Potential excess of r-process ^{130}Te

Previous leaching studies of carbonaceous chondrites revealed isotopic anomalies for several elements (K, Cr, Mo, Ba, Zr, and potentially for W), which are about one to two orders of magnitude larger than the possible ^{130}Te excess for the nitric acid leachate of Murchison-a (Rotaru et al., 1992; Podosek et al., 1997a, 1999; Dauphas et al., 2002a, 2004a; Hidaka et al., 2003; Schönbächler et al., 2003, 2005). In addition, no anomalies in the abundance of *p*-process and *s*-process Te nuclides were observed in this study, with the exception of two samples that display slightly negative values for $\varepsilon^{122}Te$ (HF–HCl leachate of Murchison-a) and $\varepsilon^{124}Te$ (50% HAc leachate of Orgueil), (Fig. 4, Table 2). There are a number of other elements that do not display isotope anomalies in similar leaching experiments either, including Ca, Ti, Fe, Ni, Zn, Se, Rb, and Sr (Rotaru et al., 1992; Podosek et al., 1997b; Dauphas et al., 2003; Plagge et al., 2003). This leads to the question of why the leachates of carbonaceous chondrites display large isotope anomalies for some elements, whereas others are isotopically normal.

It has been suggested that most of the nucleosynthetic isotope anomalies determined for leachates of carbonaceous chondrites reflect the presence of known (Alexander, 2002; Dauphas et al., 2002a; Schönbächler et al., 2005) or unidentified (Podosek et al., 1997a, 1999; Alexander, 2002; Schönbächler et al., 2003, 2005) presolar phases. These phases exhibit large isotopic anomalies for some of the elements that are present at high concentrations, whereas they may not host significant budgets of isotopically anomalous components for others (Rotaru et al., 1992). Such differences probably reflect mainly the different production sites of the presolar components and their chemical composition. This can also explain why nucleosynthetic anomalies are only revealed for certain elements during stepwise leaching of carbonaceous chondrites. In this respect, it is significant that the presolar Te isotope signatures of nanodiamonds (Maas et al., 2001) are, on average, less extreme than the Ba, Mo, and Zr isotope anomalies of presolar silicon carbide (SiC) and graphite grains (Ott and Begemann, 1990; Zinner et al., 1991; Nicolussi et al., 1997, 1998a,b). Moreover, the latter types of presolar grains have unknown Te isotope compositions, but they are either not very extreme and / or the grains contain only tiny amounts of Te. This conclusion is strongly supported by data for the last Orgueil leach step (5b). This fraction exhibits an $\varepsilon^{96}Zr$ anomaly of $-38‰$ (Schönbächler et al., 2005), which is likely due to the presence of SiC grains, but the Te isotope composition is not anomalous.

The apparent lack of Te isotope anomalies is most likely due to the high volatility of this element, which hampered condensation into presolar SiC. It is also possible that larger Te anomalies existed in presolar phases, but they were subsequently erased or diluted by thermal metamorphism and aqueous alteration within the solar system. This would imply that the presolar carrier phases of Te were more susceptible to such processes than SiC. Alternatively, it is conceivable that Te was volatilized in the solar nebula, leading to relatively efficient homogenization of any pre-existing anomalies.

Assuming that the ^{130}Te excesses of the leachates are real, the most straightforward explanation is the presence of an *r*-process component. As both ^{130}Te and ^{128}Te are produced solely by the *r*-process, it is reasonable to expect

correlated anomalies for these two isotopes. It is thus important that the small positive $\varepsilon^{130}Te_{56}$ anomalies of some leachates are always accompanied by small positive $\varepsilon^{128}Te_{56}$ values (Fig. 4, Table 2), even though the latter are, within error, identical to the standard. The ideal normalization ratio for the detection of correlated anomalies in ^{130}Te and ^{128}Te would utilize ^{122}Te and ^{124}Te, as the latter are both exclusively produced by the *s*-process. However, the use of this normalization pair results in uncertainties of ± 4.3 ε units for $(^{128}Te/^{124}Te)_{24}$ and ± 6 ε for $(^{130}Te/^{124}Te)_{24}$, for the analysis of the Murchison-a HNO_3 leachate. With this precision, no deviations in Te isotope compositions are resolvable. The use of ^{125}Te as the reference isotope and $^{125}Te/^{126}Te$ for mass-bias correction provides superior precision. Synthetic spectra, which were calculated for *r*-process excesses, furthermore reveal coupled anomalies in $\varepsilon^{128}Te_{56}$ and $^{130}Te_{56}$, even though ^{125}Te and ^{126}Te are produced by both the *s*- and *r*-process (Table 2, Fig. 4). The $^{130}Te/^{128}Te$ ratio measured in presolar diamonds of Allende by Maas et al. (2001) is 2.5 ± 1.2. For $\varepsilon^{130}Te_{56} = +3.5$ as deduced for the HNO_3-leachate of Murchison-a, this would imply an expected $\varepsilon^{128}Te_{56}$ of about +1.5. This prediction is in accord with the Te isotope data obtained in this study (Table 2). In contrast, Richter et al. (1998) measured a $^{130}Te/^{128}Te$ of about 0.98 in presolar diamonds of Allende, which is significantly lower. Given the relatively large uncertainties, the data of Richter et al. (1998) are also in agreement with the results of the present study, however.

The occurrence of the ^{130}Te excesses shows no systematic pattern in the leached meteorites. This could be a result of the small magnitude of the excesses and it is, therefore, highly tentative to argue about the nature of potential carrier phases. It seems quite unlikely that presolar diamonds, which host anomalies in the abundances of the *r*-process nuclides ^{128}Te and ^{130}Te, are attacked by the leach procedure applied in this study. However, it is unknown where Te is actually located in these nanodiamonds. Assuming that the Te of presolar diamond is not released by the presented procedure, this implies that there exists at least one additional phase that hosts an *r*-process Te component. Alternatively, the data could be explained by a very acid resistant phase with an *s*-process Te signature that generates an *s*-process deficit. The latter option is further discussed below.

Nucleosynthetic Mo isotope anomalies of leachates (and bulk samples) of carbonaceous chondrites have been interpreted to represent coupled *r*- and *p*-process anomalies or a depletion in *s*-process nuclides (Dauphas et al., 2002a,b, 2004b). No anomalies in the *p*-process isotope ^{120}Te were observed in this study (Table 2, Fig. 4). However, these measurements have large uncertainties, because ^{120}Te is the least abundant Te isotope (0.1%) and the precision of the ε^{120}Te data is in the range of the largest *p*-process Mo isotope anomaly. Nevertheless, the positive anomalies in ^{130}Te (and ^{128}Te) could also be due to a deficit in *s*-process Te. This would imply the presence of at least one phase that is enriched in *s*-process isotopes of Te and which is not preferentially digested in any of the leaching steps. For Mo and Zr it was suggested that the *s*-process components of these elements were released from presolar SiC (and/or graphite) grains (Dauphas et al., 2002a; Schönbächler et al., 2005). A similar interpretation of the Te data is considered to be unlikely, however, as it was suggested that presolar SiC grains are at least partially attacked by HCl-HF (Dauphas et al., 2002a; Schönbächler et al., 2005) and these leachates do not show an excess of *s*-process Te isotopes. Furthermore, it is presently not known if such grains contain significant amounts of Te with anomalous isotopic compositions. Since SiC grains are refractory high-temperature phases, only refractory elements are expected to condense into them. Therefore, Te might be too volatile to be incorporated into these grains. Older analyses of acid-etched residues of Allende that are likely to be enriched in presolar SiC and graphite, displayed no Te isotope anomalies, but these measurements were only precise to about ± 2 to $\pm 3‰$ for $^{125}Te/^{130}Te$, $^{126}Te/^{130}Te$, and $^{128}Te/^{130}Te$ because they were conducted on very small samples by thermal ionization mass spectrometry (Loss et al., 1990). Furthermore, Allende has a very low abundance of presolar SiC grains. It is also notable in this context, that the *r*-process Te component of Allende presolar diamonds requires no complementary *s*-process material to be present, as the contribution of the former to the total Te budget of carbonaceous chondrites is insignificant and the isotope compositions of this material does not appear to be extreme (Fehr et al., 2005).

3.4. Conclusions

Leachates of the carbonaceous chondrites Orgueil, Murchison, and Allende do not display radiogenic or large nucleosynthetic Te isotope anomalies. There is a hint of small excesses of about 0.3–0.4‰ for the *r*-process nuclide ^{130}Te. Compared to the effects determined for ^{54}Cr, ^{40}K, Mo, Ba, and ^{96}Zr in similar leachates, the ^{130}Te excesses are one to two orders of magnitude smaller. Any potential ^{126}Te anomalies from the decay of ^{126}Sn are too small to be resolvable or absent. The upper limit for the initial $^{126}Sn/^{124}Sn$ ratio, as deduced from the invariance of the atomic abundance of ^{126}Te with Sn/Te for all leachate data, is 7.7×10^{-5}. How close this is to the initial $^{126}Sn/^{124}Sn$ ratio of the solar system depends on when the investigated samples last experienced redistribution of Sn and Te.

In order to continue the search for ^{126}Te anomalies, it will be necessary to identify phases with high Sn/Te ratios that formed very early in the solar system. In addition, these phases need to be undisturbed by later alteration processes and metamorphism. Possible candidates are calcium–aluminum-rich inclusions (CAI's), which are thought to be the first solids formed in the solar system and that are known to be the host of many anomalies from the decay of short-lived radionuclides. Some CAI's have Sn concentrations of 1 ppm and more (Mason and Martin, 1977) and possibly possess high

Sn/Te ratios. However, they have to be selected with caution, because numerous CAI's of oxidized CV3 carbonaceous chondrites have experienced severe alteration (Krot et al., 1995). In addition, it would be desirable to investigate whether presolar SiC and graphite grains have anomalous Te isotope compositions that could be responsible for the small ^{130}Te excesses observed for leachates of carbonaceous chondrites.

Acknowledgements

We thank Der-Chuen Lee, Glenn J. MacPherson, Don Porcelli, Sarah Woodland, and Brigitte Zanda for helpful discussions. Glenn J. MacPherson (USNW-6159 and USNW-5459) and Brigitte Zanda are furthermore acknowledged for providing samples from the collections of the Smithsonian Institution of Washington and the Natural History Museum in Paris, respectively. Tomáš Magna is thanked for performing some measurements with a quadrupole ICPMS for interference checks. Moreover, we would like to acknowledge Bob Loss, Ernst Zinner, and an anonymous reviewer whose comments significantly improved the manuscript. We are particularly indebted to the anonymous reviewer, whose calculations regarding the initial ^{126}Sn abundances were included in the final version of this manuscript. Noriko Kita is thanked for her prompt editor handling. Financial support was provided by the ETH Zürich Forschungskommission and the Schweizerische Nationalfonds (SNF).

Associate editor: Noriko Kita

References

Alexander, C.M.O'D., 2002. The carrier of the ^{54}Cr anomaly—ubiquitous and uniform in composition. *Lunar Planet. Sci.* **33**, 1872.

Allen Jr., R.O., Mason, B., 1973. Minor and trace elements in some meteoritic minerals. *Geochim. Cosmochim. Acta* **37**, 1435–1456.

Arlandini, C., Käppeler, F., Wisshak, K., 1999. Neutron capture in low-mass asymptotic giant branch stars: cross sections and abundance signatures. *Astrophys. J.* **525**, 886–900.

Bischoff, A., 1998. Aqueous alteration of carbonaceous chondrites—a review. *Meteor. Planet. Sci.* **33**, 1113–1122.

Bourot-Denise, M., Zanda, B., Hewins, R.H., 1997. Metamorphic transformation of opaque minerals in chondrites. In: Zolensky, M.E., Krot, A.N., Scott, E.R.D. (Eds.), Workshop on parent-body and nebular modification of chondritic materials. LPI Technical Report Number 97-02, Part 1, 5–7.

Brearley A.J., 2004. Nebular versus parent body processing. In: Holland, H.D., Turekian, K.K. (Eds.), Davis, A. (Vol. Ed.), Treatise on Geochemistry, vol. 1, Elsevier, Amsterdam, pp. 247–268.

Brearley, A.J., Jones, R.H., 1998. Chondritic meteorites. In: Papike, J.J. (Ed.), Planetary Materials, vol. 36, Reviews in Mineralogy, Mineral. Soc. America, pp. 1–398.

Bullock, E.S., Gounelle, M., Lauretta, D.S., Grady, M.M., Russell, S.S., 2005. Mineralogy and texture of Fe-Ni sulfides in CI1 chondrites: Clues to the extent of aqueous alteration on the CI1 parent body. *Geochim. Cosmochim. Acta* **10**, 2687–2700.

Burgess, R., Wright, I.P., Pillinger, C.T., 1985. Sulphur isotope measurements of meteorites by stepped combustion. *Lunar Planet. Sci.* **16**, 99–100.

Burgess, R., Wright, I.P., Pillinger, C.T., 1991. Determination of sulphur-bearing components in C1 and C2 chondrites by stepped combustion. *Meteoritics* **26**, 55–64.

Buseck, P.R., 1970. Tin (50). In: Mason, B. (Ed.), *Handbook of Elemental Abundances in Meteorites*, vol. 1. Science Publishers, Inc., Gordon and Breach, pp. 377–386.

Busso, M., Gallino, R., Wasserburg, G.J., 2003. Short-lived nuclei in the early solar system: a low mass stellar source? *Publ. Astron. Soc. Aust.* **20**, 356–370.

Cameron, A.G.W., Truran, J.W., 1977. The supernova trigger for formation of the solar system. *Icarus* **30**, 447–461.

Chevalier, R.A., 2000. Young circumstellar disks near evolved massive stars and supernovae. *Astrophys. J.* **538**, L151–L154.

Dauphas, N., Marty, B., Reisberg, L., 2002a. Molybdenum nucleosynthetic dichotomy revealed in primitive meteorites. *Astrophys. J.* **569**, L139–L142.

Dauphas, N., Marty, B., Reisberg, L., 2002b. Molybdenum evidence for inherited planetary scale isotope heterogeneity of the protosolar nebula. *Astrophys. J.* **565**, 640–644.

Dauphas, N., Rouxel, O., Davis, A.M., Lewis, R.S., Wadhwa, M., Marty, B., Reisberg, L., Janney, P.E., Zimmermann, C., 2003. Iron and selenium isotope homogeneity in the protosolar nebula? *Lunar Planet. Sci.* **34**, 1807.

Dauphas, N., Foley, N., Wadhwa, M., Davis, A.M., Göpel, C., Birck, J.-L., Janney, P.E., Gallino, R., 2004a. Testing the homogeneity of the solar system for iron (54, 56, 57, and 58) and tungsten (182, 183, 184, and 186) isotope abundances. *Lunar Planet. Sci.* **35**, 1498.

Dauphas, N., Davis, A.M., Marty, B., Reisberg, L., 2004b. The cosmic molybdenum-ruthenium isotope correlation. *Earth Planet. Sci. Lett.* **226**, 465–475.

Fehr, M.A., Rehkämper, M., Halliday, A.N., 2004. Application of MC-ICPMS to the precise determination of tellurium isotope compositions in chondrites, iron meteorites and sulfides. *Int. J. Mass Spectrom.* **232**, 83–94.

Fehr, M.A., Rehkämper, M., Halliday, A.N., Wiechert, U., Hattendorf, B., Günther, D., Ono, S., Eigenbrode, J.L., Rumble III, D., 2005. The tellurium isotopic composition of the early solar system—a search for isotope anomalies from the decay of ^{126}Sn, stellar nucleosynthesis, and mass independent fractionations. *Geochim. Cosmochim. Acta* **69**, 5099–5112.

Fredriksson, K., Kerridge, J.F., 1988. Carbonates and sulfates in CI chondrites: formation by aqueous activity on the parent body. *Meteoritics* **23**, 35–44.

Goles, G.G., Anders, E., 1962. Abundances of iodine, tellurium and uranium in meteorites. *Geochim. Cosmochim. Acta* **26**, 723–737.

Gounelle, M., Zolensky, M.E., 2001. A terrestrial origin for sulfate veins in CI1 chondrites. *Meteorit. Planet. Sci.* **36**, 1321–1329.

Grossman, J.N., 2002. The redistribution of sulfides during metamorphism and alteration of primitive chondrites. *Meteorit. Planet. Sci.* **37**, A57.

Hamaguchi, H., Kuroda, R., 1969. Tin: 50-D. Abundance in rock-forming minerals (I), tin minerals (II), phase equilibria (III). In: Wedepohl, K.H. (Ed.), *Handbook of Geochemistry*, vol. 2. Springer-Verlag, Berlin.

Hanson, M.W., Bradbury, W.C., Carlton, J.K., 1957. Spectrophotometric determination of tellurium. *Anal. Chem.* **29**, 490–491.

Hidaka, H., Ohta, Y., Yoneda, S., 2003. Nucleosynthetic components of the early solar system inferred from Ba isotopic compositions in carbonaceous chondrites. *Earth Planet. Sci. Lett.* **214**, 455–466.

Hyman, M., Rowe, M.W., Herndon, J.M., 1979. Magnetite heterogeneity among CI chondrites. *Geochem. J.* **13**, 37–39.

Hyman, M., Rowe, M.W., 1983. Magnetite in CI chondrites. *Lunar Planet. Sci.* **34**, 341–342.

Ikramuddin, M., Matza, S., Lipschutz, M.E., 1977. Thermal metamorphism of primitive meteorites—V. Ten trace elements in Tieschitz H3 chondrite heated at 400–1000 °C. *Geochim. Cosmochim. Acta* **41**, 1247–1256.

Johnson, W.M., Maxwell, J.A., 1981. *Rock and Mineral Analysis*. Wiley, New York.

Krot, A.N., Scott, E.R.D., Zolensky, M.E., 1995. Mineralogical and chemical modification of components in CV3 chondrites: Nebular or asteroidal processing? *Meteoritics* **30**, 748–775.

Lauretta, D.S., Lodders, K., Fegley Jr. B., 1997a. The alteration of nickel-bearing sulfides during thermal metamorphism on ordinary chondrite parent bodies. In: Zolensky, M.E., Krot, A.N., Scott, E.R.D. (Eds.), Workshop on parent-body and nebular modification of chondritic materials. LPI Technical Report Number 97-02, Part 1, 36–38.

Lauretta, D.S., Lodders, K., Fegley Jr., B., 1997b. Experimental simulations of sulfide formation in the solar nebula. *Science* **277**, 358–360.

Lauretta, D.S., Klaue, B., Blum, J.D., 2002. Thermal analysis of volatile trace elements in carbonaceous and ordinary chondrites. *Lunar Planet. Sci.* **33**, 1602.

Lee, D.-C., Halliday, A.N., 1995. Precise determinations of the isotopic compositions and atomic weights of molybdenum, tellurium, tin and tungsten using ICP magnetic sector multiple collector mass spectrometry. *Int. J. Mass Spectrom. Ion. Process* **146/147**, 35–46.

Lee, T., Shu, F.H., Shang, H., Glassgold, A.E., Rehm, K.E., 1998. Protostellar cosmic rays and extinct radioactivities in meteorites. *Astrophys. J.* **506**, 898–912.

Leutwein, F., 1972. Tellurium: 52-D. Abundance in rock-forming minerals; Tellurium minerals. In: Wedepohl, K.H. (Ed.), *Handbook of Geochemistry*, vol. 2. Springer-Verlag, Berlin.

Lin, Y.T., Guan, Y.B., Leshin, L.A., Quayang, Z.Y., Wang, D., 2005. Short-lived chlorine-36 in a Ca- and Al-rich inclusion from the Ningqiang carbonaceous chondrite. *Proc. Nat. Acad. Sci. USA* **102**, 1306–1311.

Lodders, K., 2003. Solar system abundances and condensation temperatures of the elements. *Astrophys. J.* **591**, 1220–1247.

Loss, R.D., Rosman, K.J.R., De Laeter, J.R., 1990. The isotopic composition of zinc, palladium, silver, cadmium, tin and tellurium in acid-etched residues of the Allende meteorite. *Geochim. Cosmochim. Acta* **54**, 3525–3536.

Maas, R., Loss, R.D., Rosman, K.J.R., De Laeter, J.R., Lewis, R.S., Huss, G.R., Lugmair, G.W., 2001. Isotope anomalies in tellurium and palladium from Allende nanodiamonds. *Meteorit. Planet. Sci.* **36**, 849–858.

Mason, B., Graham, A.L., 1970. Minor and trace elements in meteoritic minerals. *Smith. Contrib. Earth Sci.* **3**, 84–95.

Mason, B., Martin, P.M., 1977. Geochemical differences among components of the Allende meteorite. In: Mason, B. (Ed.), Mineral Sciences Investigations, 1974–1975, vol. 19, Smith. Contrib. Earth Sci., pp. 84–95.

Matza, S., Lipschutz, M.E., 1977. Thermal metamorphism of primitive meteorites—VI. Eleven trace elements in Murchison C2 chondrite heated at 400–1000 °C. *Proc. Eight Lunar Sci. Conf.* **8**, 161–176.

Matza, S., Lipschutz, M.E., 1978. Thermal metamorphism of primitive meteorites—VII. Mineralogy–petrology of heated Murchison (C2) and alteration of C30 and other chondrites. *Geochim. Cosmochim. Acta* **42**, 1655–1667.

Meyer, B.S., Clayton, D.D., 2000. Short-lived radioactivities and the birth of the Sun. *Space Sci. Rev.* **92**, 133–152.

Meyer, B.S., The, L.-S., Clayton, D.D., 2004. Helium-shell nucleosynthesis and extinct radioactivities. *Lunar Planet. Sci.* **35**, 1908.

Nicolussi, G.K., Davis, A.M., Pellin, M.J., Lewis, R.S., Clayton, R.N., Amari, S., 1997. s-process zirconium in presolar silicon carbide grains. *Science* **277**, 1281–1283.

Nicolussi, G.K., Pellin, M.J., Lewis, R.S., Davis, A.M., Amari, S., Clayton, R.N., 1998a. Molybdenum isotopic composition of individual presolar silicon carbide grains from the Murchison meteorite. *Geochim. Cosmochim. Acta* **62**, 1093–1104.

Nicolussi, G.K., Pelin, M.J., Lewis, R.S., Davis, A.M., Clayton, R.N., Amari, S., 1998b. Zirconium and molybdenum in individual circumstellar graphite grains: new isotopic data on the nucleosynthesis of heavy elements. *Astrophys. J.* **504**, 492–499.

Noll Jr., P.D., Newsom, H.E., Leeman, W.P., Ryan, J.G., 1996. The role of hydrothermal fluids in the production of subduction zone magmas: evidence from siderophile and chalcophile trace elements and boron. *Geochim. Cosmochim. Acta* **60**, 587–611.

Oberli, F., Gartenmann, P., Meier, M., Kutschera, W., Suter, M., Winkler, G., 1999. The half-life of ^{126}Sn refined by thermal ionization mass spectrometry measurements. *Int. J. Mass Spectrom.* **184**, 145–152.

Ott, U., Begemann, F., 1990. Discovery of s-process barium in the Murchison meteorite. *Astrophys. J.* **353**, L57–L60.

Ouellette N., Desch S.J., Hester J.J., Leshin L.A., 2005. A nearby supernova injected short-lived radionuclides into our protoplanetary disk. In: Chondrites and the Protoplanetary Disk, ASP Conf. Series 341, 527–538.

Plagge, M., Sudek, C., Ott, U., 2003. Selenium during stepwise dissolution of Allende—an exploration study. *Lunar Planet. Sci.* **34**, 1217.

Podosek, F.A., Ott, U., Brannon, J.C., Neal, C.R., Bernatowicz, T.J., Swan, P., Mahan, S.E., 1997a. Thoroughly anomalous chromium in Orgueil. *Meteorit. Planet. Sci.* **32**, 617–627.

Podosek, F.A., Nichols, R.H., Brannon, J.C., Ott, U., 1997b. Is only Cr thoroughly anomalous in carbonaceous chondrites? *Lunar Planet. Sci.* **28**, 1695.

Podosek, F.A., Nichols Jr., R.H., Brannon, J.C., Meyer, B.S., Ott, U., Jennings, C.L., Luo, N., 1999. Potassium, stardust, and the last supernova. *Geochim. Cosmochim. Acta* **63**, 2351–2362.

Qian, Y.-Z., Vogel, P., Wasserburg, G.J., 1998. Supernova as the site of the r-process: implications for gamma-ray astronomy. *Astrophys. J.* **506**, 868–873.

Reed, G.W., Allen, R.O.J., 1966. Halogens in chondrites. *Geochim. Cosmochim. Acta* **30**, 779–800.

Richter, S., Ott, U., Begemann, F., 1998. Tellurium in pre-solar diamonds as an indicator for rapid separation of supernova ejecta. *Nature* **391**, 261–263.

Rietmeijer, F.J., 1989. Tin in a chondritic interplanetary dust particle. *Meteoritics* **24**, 43–47.

Rotaru, M., Birck, J.L., Allègre, C.J., 1992. Clues to early solar system history from chromium isotopes in carbonaceous chondrites. *Nature* **358**, 465–470.

Russell, S.S., Gounelle, M., Hutchinson, R., 2001. Origin of short-lived radionuclides. *Philos. Trans. R. Soc. Lond. A* **359**, 1991–2004.

Schönbächler, M., Lee, D.-C., Rehkämper, M., Halliday, A.N., Fehr, M.A., Hattendorf, B., Günther, D., 2003. Zirconium isotope evidence for incomplete admixing of *r*-process components in the solar nebula. *Earth Planet. Sci. Lett.* **216**, 467–481.

Schönbächler, M., Rehkämper, M., Lee, D.-C., Halliday, A.N., 2004. Ion exchange chromatography and high precision isotopic measurements of zirconium by MC-ICPMS. *Analyst* **129**, 32–37.

Schönbächler, M., Rehkämper, M., Fehr, M.A., Halliday, A.N., Hattendorf, B., Günther, D., 2005. Nucleosynthetic zirconium isotope anomalies in acid leachates of carbonaceous chondrites. *Geochim. Cosmochim. Acta* **69**, 5113–5122.

Shima, M., 1964. The distribution of germanium and tin in meteorites. *Geochim. Cosmochim. Acta* **28**, 517–532.

Yi, W., Halliday, A.N., Lee, D.-C., Christensen, J.N., 1995. Indium and tin in basalts, sulfides, and the mantle. *Geochim. Cosmochim. Acta* **59**, 5081–5090.

Zanda B., Yu, Y., Bourot-Denise M., and Hewins R.H., 1997. The history of metal and sulfides in chondrites. In: Zolensky, M.E., Krot, A.N., Scott, E.R.D. (Eds.), Workshop on parent-body and nebular modification of chondritic materials. LPI Technical Report Number 97-02, Part 1, 68–70.

Zinner, E., Amari, S., Lewis, R.S., 1991. s-process Ba, Nd, and Sm in presolar SiC from the Murchison meteorite. *Astrophys. J.* **382**, L47–L50.

Zolensky, M., McSween Jr., H.J., 1988. Aqueous alteration. In: Kerridge, J.F., Matthews, M.S. (Eds.), *Meteorites and the Early Solar System*. University of Arizona Press, NY, pp. 114–143.